Highly convergent dynamic models obtained by modal synthesis with application to short wave pulse propagation

Rimantas Barauskas*,† and Ramute Barauskiene

Department of System Analysis, Kaunas University of Technology, Lithuania

SUMMARY

A general approach for obtaining the matrices of a substructure ensuring minimum modal frequency errors of the whole structure is presented. The mass and stiffness matrices of a small component domain of selected dimension are obtained by applying the modal synthesis of a limited number of close-to-exact modes such that after assembling a larger joined domain model the modal convergence rate of the latter should be as high as possible. The goal is achieved by formulating the minimization problem for the penalty-type target function representing the cumulative relative modal frequency error of the joined sample domain and by applying the gradient descent minimization method. After the optimum matrices of a component domain are obtained, they can be used in any structure as higher-order elements or super-elements. The well-known generalized mass matrices obtained as a weighted sum of lumped and consistent components can be treated as a special case of the presented approach. The obtained dynamic models are used for modelling short transient waves and wave pulses propagating in elastic or acoustic environments by using a only a few nodal points per pulse length. Copyright © 2004 John Wiley & Sons, Ltd.

KEY WORDS: modal synthesis; modal error; wave propagation

1. INTRODUCTION

Computer simulation of wave propagation processes is of key importance for solution of very different engineering problems. As one of many applications, the wave propagation modelling is widely used during development of ultrasonic measurement schemes and procedures in order to get insight into wave propagation and transformation phenomena taking place inside of the analysed domain. Identification and recognition of internal defects in continuous structures or detection of impurity particles or coagulation centres in liquids can be mentioned as ultrasonic measurement application examples where frequencies from 20–30 kHz to 3–5 MHz may be used. Computer modelling of such wave processes presents an important and challenging application field in computational mechanics as the short wavelength causes some modelling difficulties. In this work the term 'short wavelength' is used in order to indicate that the length of the wave

---
*Correspondence to: R. Barauskas, Department of System Analysis, Kaunas University of Technology, Lithuania.
†E-mail: rimantas.barauskas@mf.ktu.lt

or pulse is many times less than the dimensions of the domain in which it is propagating. For example, the problems of practical value encountered in simulations of ultrasonic measurement processes require the product (wave number) × (characteristic dimension of the domain) to be near to 100 or even 1000.

The propagating short wavelength pulse simulated in a discrete mesh is inevitably distorted. The amount of distortion grows rapidly as the distance travelled by the pulse comprises a considerable number of lengths of the pulse. An important source of the distortions of the pulse shape seems to be the phase error produced by the model. For example, in linear models different harmonic components of a longitudinal wave are travelling with slightly different phase velocities, though in the exact mathematical model the phase velocities of all the components are assumed to be the same. Such phase errors produced by the discrete model are highly undesirable as after some propagation distance the shape and duration of the simulated pulse become very different from the values expected theoretically. The consequences of amplitude errors upon the overall performance of the model are not so crucial, though also undesirable. The phase and amplitude errors produced by the model can be and usually are minimized by using very dense meshes. However, this makes the simulation complex and requires huge computational resources. The main difficulties arising in ultrasonic measurement process simulation are caused by: (a) computational models of very large dimensionality (the smallest 2D problems of any practical value require to use models consisting of 10^6–10^7 elements); (b) very large number of time integration steps (inversely proportional to the linear dimension of elements); (c) adequacy of finite elements models in representing continuum wave propagation problems.

This work intends to develop an approach enabling to reduce the phase errors produced by discrete wave propagation models. Obviously, the errors will be reduced if all the modes of the continuous domain the frequencies of which are close to spectral components of the wave pulse are represented correctly by the discrete model of the domain. In other words, the refinement of the model has to be dense enough to ensure the convergence of the above mentioned modes. If the convergence of necessary modes could be achieved in a mesh having less nodal points, such a rough mesh could be used for modelling the short wave propagation with no losses in accuracy.

As early as 1982 different modal frequency convergence features of dynamic models obtained by using lumped and consistent forms of mass matrices have been noticed [1]. However, only during the last decade this problem has been examined more thoroughly and practical recommendations regarding the form of the mass matrix have been presented. The simplest way to improve the convergence of modal frequencies of dynamic models is to use the 'generalized' form of the mass matrix obtained as a weighted superposition of the two traditional forms, [2]. In Reference [3] the dispersion effects of discrete solutions of propagating waves have been analysed with the consistent, lumped and higher-order mass matrices. The penta-diagonal mass matrix with reduced coupling has been obtained yielding improved phase and group errors, and the generalized mass matrix has been shown to improve the dispersion characteristics of both the reduced and full integration elements. The resulting mass matrices are non-diagonal, however, considerable savings are obtained because of the possibility to use elements of larger linear dimensions. Approaches concentrating on improvement of modal convergence properties and retaining the diagonal form of the mass matrix have been presented as well [4–7]. The basic idea was the re-distribution of the amounts of mass between the diagonal entries of higher order elements.

Modal synthesis is a modelling technique permitting a complex structure to be represented by a reduced number of degrees of freedom (DOF). In most cases, the substructures are described in terms of a limited number of modal displacements and subsequently the coupled system of equations describing all the structure is obtained. The problem is that by direct coupling of modes of free substructures, the modal convergence of the resulting dynamic model of the whole structure is not always good. Appropriate methods of substructure coupling have been developed [8],[9]. As a special case, modal synthesis may be used in order to obtain the matrices of elements or substructures having the prescribed dynamic properties.

Generally, the non-diagonal mass matrices can be designed to produce models of higher modal convergence rate than the diagonal ones. They require more computational effort to obtain the transient solution by means of integration of the dynamic equations. However, the total efficiency of the scheme improves as the required time step size becomes also greater with the increase of the size of elements. By selecting the appropriate form of structural matrices, the time step ensuring stability of an explicit integration scheme may become 2–5 times larger as it was necessary when the models were based on the lumped mass matrix. In this way the accuracy requirement and not the algorithmic stability governs the time step size selection.

This work presents a systematic way for obtaining the mass and stiffness matrices by modal synthesis of a limited number of exact modes of a free component domain. In reality, analytical expressions of exact modes are available only for domains of simple geometric forms. However, more complex sub-domain shapes may be used as well by obtaining their lower modes in a highly refined mesh. Such modes may be reasonably assumed to be 'exact' if we use this word in an engineering sense rather than in the purely mathematical sense. Subsequently, the word 'exact mode' in this paper is being used to characterize modes the error of which is small enough and practically may be disregarded in this application.

A certain number of modal shapes corresponding to exact modal frequencies are projected on a rough mesh the number of DOF of which is equal to the number of the exact modal frequencies available. The way the modal shapes can be projected upon a rough mesh is not unique, and a proper method of approximation ensures the optimum result. The requirement is to obtain the matrices of a small component domain of selected dimension such that after assembling the component domain matrices to a larger model the convergence of modal frequencies of the latter should be as high as possible. The goal is achieved by formulating the minimization problem for the penalty function representing the modal frequency error of the sample domains and by applying the gradient method in order to minimize it. After the optimum matrices of a component domain are obtained, they can be used in any structure as higher-order elements or super-elements.

2. LUMPED, CONSISTENT AND GENERALIZED MASS MATRICES

Finite element models of small vibrations and waves in elastic or acoustic continua are presented by the well known semi-discrete structural dynamic equation as

$$[\mathbf{M}]\{\ddot{\mathbf{U}}\} + [\mathbf{C}]\{\dot{\mathbf{U}}\} + [\mathbf{K}]\{\mathbf{U}\} = \{\mathbf{R}(t)\} \qquad (1)$$

where $[\mathbf{M}]$, $[\mathbf{K}]$—structural mass and stiffness matrices of the element, $\{\mathbf{R}\}$—nodal vector containing the lumped forces. In problems addressed in this work we assume the damping forces to be very small. If necessary, slight damping can be conveniently introduced by means

of the proportional damping matrix $[\mathbf{C}] = \alpha[\mathbf{M}] + \beta[\mathbf{K}]$. The reason for such a simplification is that in many ultrasonic measurement applications propagating pulses do not fade perceptibly after travelling distances considered by simulations, as well as, the investigations are mainly focused on the wave type transformations caused by reflections and interactions. Further in this work we neglect the damping forces completely by taking $\alpha = \beta = 0$.

When using explicit techniques for solving Equation (1), ~ 17 mesh points per wavelength of the highest harmonic component are generally recommended [10]. It can be easily demonstrated that after travelling a distance of 20–50 pulse lengths the error in time of arrival and amplitude of the pulse, as well as, the percentage of the amplitude of the leading and (or) lagging numerical noise related to the amplitude of the pulse do not exceed 3–5%. Such solutions of a propagating wave pulse can often be regarded as 'practically acceptable'.

The latter estimation is valid for models with the 'lumped' (diagonal) version of the mass matrix obtained by distributing the element mass in equal portions between the nodes of the element. Very similar element size estimation is valid for consistent mass matrices. Though consistent mass matrix models usually give better convergence for lower modes, the convergence of higher modes is not significantly better as in the case of the lumped mass matrix. Therefore, in practice lumped mass matrices are commonly used as requiring less computational resource by using explicit time integration numerical schemes.

It is well known that lumped mass matrices $[\mathbf{M}_L^e]$ have a tendency to produce diminished values of all modal frequencies. On the contrary, consistent mass matrices $[\mathbf{M}_C^e]$ produce enlarged modal frequency values in the lower and mid-frequency range. The optimum choice often is the generalized mass matrix obtained as the weighted sum of the two. Fundamental results on this topic have been summarized in Reference [11] proving that the weights of $k_C = k_L = 0.5$ for both the consistent and the lumped mass matrices enable to obtain the 'higher order' mass matrix. However, the best results can be obtained by selecting the weights in accordance with the type of the element and also slightly depends upon the character of the problem solved. In this work we obtained that nearly minimum distortions of a uni-dimensional propagating wave pulse after travelling considerable distances can be obtained by applying weights $k_C = 0.53$; $k_L = 0.47$. For rectangular elements of the two-dimensional acoustic problem our choice has been $k_C = 0.7$; $k_L = 0.3$, as it will be discussed later in Section 5 of this work. Such values k_C; k_L do not pretend to have a strict theoretical background, however, they can be recommended on the base of visual inspections of obtained solutions of typical propagating signals. As also we demonstrate in the following discussions, the 'nearly optimal' choice of k_C; k_L has not necessarily to minimize the total modal frequency error. Often it appears as preferable to minimize the error over a certain frequency range of the modal spectrum specific for one or another class of problems. Practically, by using the generalized mass matrix the performance of the model can be improved significantly. As a result, the linear dimension of the element can be increased to 3–5 times in comparison with the element dimensions required by the lumped mass matrix models. A deeper numerical study is presented further in Sections 5.1 and 5.2.

3. MATRICES OF DOMAINS OBTAINED BY MODAL SYNTHESIS

The quality of performance of transient short wave propagation models depends heavily upon the convergence rate of modal frequencies over all range, including mid-frequency and higher modes of the domain.

Definition

An 'ideal' $n \times n$ discrete model of wave propagation in a closed domain represents the modal frequencies of all n modes close enough to exact modal frequencies of the continuous domain of the same shape. Moreover, the correct representation of all n modal frequencies should be satisfied for any value of n.

Under such condition the 'wavelength against frequency' relationship ('the dispersion characteristic') of the discrete model of a linear domain is a straight line and the model is able to represent the maximum number of spectral components of the investigated propagating wave package correctly. Unfortunately, in reality the problem of making the model close to 'ideal' is not simple and, may be, it is impossible to satisfy exactly the requirements posed in the above mentioned definition. However, discrete models presenting good approximations to 'ideal' ones can be built. Their matrices are non-diagonal, however, the element sizes can be increased significantly.

Consider an unconstrained elastic or acoustic domain meshed uniformly and presented by structural matrices of dimension $N \times N$ as $[\mathbf{M}]_{N \times N}$, $[\mathbf{K}]_{N \times N}$. In the following we call it the 'original model'. By solving the eigenvalue problem we obtain modal frequencies $\omega_1, \omega_2, \ldots, \omega_N$ and modal shapes $[\mathbf{Y}] = [\{\mathbf{y}_1\}, \{\mathbf{y}_2\}, \ldots, \{\mathbf{y}_N\}]$. Assume that first n modal frequencies are good enough approximations to their exact values, however, $n \ll N$. Now we build a new 'rough model' of dimension $n \times n$ of the same domain. The matrices of the rough model possessing all n values of natural frequencies equal to those calculated from the original model can be obtained by using modal synthesis technique as

$$[\tilde{\mathbf{M}}] = ([\tilde{\mathbf{Y}}]^{\mathrm{T}})^{-1}[\tilde{\mathbf{Y}}]^{-1} = [\mathbf{M}][\tilde{\mathbf{Y}}][\tilde{\mathbf{Y}}]^{\mathrm{T}}[\mathbf{M}]$$

$$[\tilde{\mathbf{K}}] = ([\tilde{\mathbf{Y}}]^{\mathrm{T}})^{-1}[\mathrm{diag}(\omega_1^2, \omega_2^2, \ldots, \omega_n^2)]\,[\tilde{\mathbf{Y}}]^{-1} = [\mathbf{M}][\tilde{\mathbf{Y}}][\mathrm{diag}(\omega_1^2, \omega_2^2, \ldots, \omega_n^2)][\tilde{\mathbf{Y}}]^{\mathrm{T}}[\mathbf{M}] \quad (2)$$

where $\omega_1, \omega_2, \ldots, \omega_n$ are the lower modal frequencies of the original model of dimension $N \times N$, and $[\tilde{\mathbf{Y}}] = [\{\tilde{\mathbf{y}}_1\}, \{\tilde{\mathbf{y}}_2\}, \ldots, \{\tilde{\mathbf{y}}_n\}]$—the lower modal shapes of the original model approximated in the rough mesh. If the number of linearly independent modal shapes modes n and the number of DOF of the rough model are equal, $\mathrm{rank}([\tilde{\mathbf{M}}]) = n$ and no problems occur in calculating $[\tilde{\mathbf{M}}]^{-1}$ necessary for implementing the direct integration scheme.

Relations (2) ensure that all n modal frequencies of the new rough model of the domain have the values very close to exact, and, as a stand-alone model, it is 'ideal'. However, our goal is to use further the obtained model as a component domain in order to compose larger joined domains. Unfortunately, the modal frequencies of the joined domain composed of several such component domains, as a rule, will not be close to the exact values. The problem to be solved now is as follows:

Problem 1

Obtain the matrices $[\tilde{\mathbf{M}}]$, $[\tilde{\mathbf{K}}]$ of a component domain such that the joined domain of any geometric shape formed by assembling together the matrices of component domains would have as many as possible exact values of modal frequencies.

The key to the solution of Problem 1 is that the matrices synthesized by using (2) are not unique. Though we know all exact values of the modal frequencies of the rough model, the higher modal shapes in the rough mesh are not able to approximate closely the exact
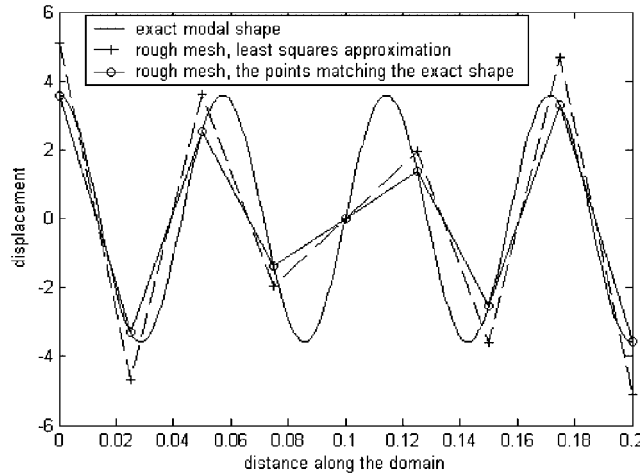
Figure 1. Approximations of the exact modal shape of 1D domain in a rough mesh.

modal shapes available in the original mesh. Rather rough approximations inevitably have to be made. In Figure 1 the explanation for the 1D case is presented that can be easily extended to 2D and 3D cases as well. The higher modal shapes sometimes are not 'correct' physically, however, they still have their influence upon the overall correctness of representation of greater wavelengths. Aliasing of short wavelength signals with longer ones does not take place because the modal synthesis relation (2) ensures the strict separation of the values of modal frequencies corresponding to longer 'physically correct' waves from the physically fictitious waves of the similar wavelength.

The least squares approximation is obtained by using the error minimum condition for ith modal shape as

$$\frac{\partial}{\partial \{\tilde{\mathbf{y}}_i^e\}} \left(\sum_{e=1}^{N_{\text{el}}} \int_{V^e} (\{\mathbf{y}_i(x,y,z)\} - [\tilde{\mathbf{N}}^e(x,y,z)]\{\tilde{\mathbf{y}}_i^e\})^{\mathrm{T}} (\{\mathbf{y}_i(x,y,z)\} - [\tilde{\mathbf{N}}^e(x,y,z)]\{\tilde{\mathbf{y}}_i^e\}) \, \mathrm{d}V \right) = 0$$

(3)

where $\{\mathbf{y}_i(x,y,z)\}$ is the displacement of point (x,y,z) on the ith exact modal shape, $\{\tilde{\mathbf{y}}_i^e\}$—displacements of ith modal shape of element e in the rough model, $[\tilde{\mathbf{N}}^e(x,y,z)]$—form functions interpolating the displacement field within element e of the rough model, N_{el}—number of elements of the rough model.

From (3) the equations for each element are obtained as

$$[\tilde{\mathbf{A}}^e]\{\tilde{\mathbf{y}}^e\} = \{\tilde{\mathbf{b}}^e\}$$

where

$$[\tilde{\mathbf{A}}^e] = \int_{V^e} [\tilde{\mathbf{N}}^e]^{\mathrm{T}} [\tilde{\mathbf{N}}^e] \, \mathrm{d}V, \quad \{\tilde{\mathbf{b}}^e\} = \int_{V^e} [\tilde{\mathbf{N}}^e]^{\mathrm{T}} \{\mathbf{y}_i(x,y,z)\} \, \mathrm{d}V$$

The element matrices $[\tilde{\mathbf{A}}^e]$, $\{\tilde{\mathbf{b}}^e\}$ are assembled in order to form the structural matrices of the entire component domain and finally ith modal shape of the rough model is obtained by solving the equation

$$[\tilde{\mathbf{A}}]\{\tilde{\mathbf{y}}_i\} = \{\tilde{\mathbf{b}}\} \tag{4}$$

The modal shapes in the rough mesh can be obtained by using different approximating functions $[\tilde{\mathbf{N}}^e]$. As the first choice we take form functions $[\tilde{\mathbf{N}}^e_c]$ of the element. In this way we take into account the interpolated displacements over all volume of the element in order to determine the approximation error (3). Alternatively, functions $[\tilde{\mathbf{N}}^e_\delta]$ may be used containing δ-functions $V_e/n_e\,\delta(x_i, y_i, z_i)$, where V_e—volume of the element, n_e—number of nodes of the element. By using $[\tilde{\mathbf{N}}^e_\delta]$ as interpolation functions, only displacements of nodes of the element are taken into account when determining the approximation error (3).

For the 1D element the above mentioned functions read as $[\tilde{\mathbf{N}}^e_c] = \left[1 - \frac{x}{l}; \ \frac{x}{l}\right]$; $[\tilde{\mathbf{N}}^e_\delta] = \left[\frac{Al}{2}\delta(0); \ \frac{Al}{2}\delta(l)\right]$. Note that $[\tilde{\mathbf{N}}^e_c]$ and $[\tilde{\mathbf{N}}^e_\delta]$ are the form functions used in consistent and lumped mass matrix formulations correspondingly, so the analogy between the two forms of error approximation and the two forms of the mass matrix is evident.

The best result is obtained by combining both types of functions as $[\tilde{\mathbf{N}}^e] = \beta_i^l[\tilde{\mathbf{N}}^e_\delta] + (1-\beta_i^l)[\tilde{\mathbf{N}}^e_c]$, where $0 < \beta_i^l < 1$ is the coefficient used for approximation of ith modal shape. In practical computation, the coefficient matrix and the right-hand side vector used in (4) have different values for each mode and are obtained by combining the consistent and lumped forms of matrix $[\tilde{\mathbf{A}}^e]$ as

$$[\tilde{\mathbf{A}}] = \beta_i^l[\tilde{\mathbf{A}}_l] + (1 - \beta_i^l)[\tilde{\mathbf{A}}_c] \tag{5}$$

and of vector $\{\tilde{\mathbf{b}}^e\}$ as

$$[\tilde{\mathbf{b}}] = \beta_i^l \frac{V_e}{n_e}\{\tilde{\mathbf{y}}_{il}\} + (1 - \beta_i^l)[\tilde{\mathbf{b}}_c] \tag{6}$$

where $[\tilde{\mathbf{A}}_c]$, $[\tilde{\mathbf{b}}_c]$—the consistent forms of the matrix and vector obtained by using approximation functions $[\tilde{\mathbf{N}}^e_c]$, $[\tilde{\mathbf{A}}_l]$—lumped form of the matrix obtained by using approximation functions $[\tilde{\mathbf{N}}^e_\delta]$, $\{\tilde{\mathbf{y}}_{il}\}$—$i$th modal shape of the rough model the displacements of which coincide with the displacements of exact modal shapes at nodal points of the rough mesh, see curve (-o-) in Figure 1.

The values of β_i^l may be selected for each ith mode individually, or the same value for all modes may be used. Anyway, the selection of β_i^l value offers a certain amount of flexibility in defining the modal shapes of the rough model and may be used as 'design parameters' in order to obtain the model of a component domain able to produce the best spectral properties of joined domains. Simultaneously, the correct physical essence of the modes approximated in the rough mesh is preserved at any value of $\beta_i^l \in [0; 1]$.

4. OPTIMUM SPECTRAL PROPERTIES OF COMPONENT DOMAINS

A joined domain obtained by assembling together 'ideal' component domains may have significant modal frequency errors. Much better spectral properties of the joined domain may

be obtained by assembling component domains that have slightly distorted modal spectrum with respect to the 'ideal' one. In following we develop a *systematic approach to optimally modify the spectral properties of a component domain in order to produce the minimum modal frequency error of joined domains*.

Consider a component domain the matrices of which are obtained by using (2). Its n modal frequencies can be presented as $0, \ldots, 0, \omega_{r+1}, \omega_{r+2}, \ldots, \omega_n$, where r—number of rigid body modes, and its n modes read as $[\tilde{\mathbf{Y}}] = [\{\tilde{\mathbf{y}}_1\}, \ldots, \{\tilde{\mathbf{y}}_r\}, \{\tilde{\mathbf{y}}_{r+1}\}, \ldots, \{\tilde{\mathbf{y}}_n\}]$. The spectral properties of the model of the domain can be slightly changed by modifying the values of modal frequencies, as well as, the modal shapes. The modifications must preserve the physical essence of the finite element model of an unconstrained domain, i.e. the lower r modal frequencies have to be zeroes, and the modal shape vectors have to be orthogonal and express essentially the same shapes as before the modification. Also the total mass of the domain must remain unchanged.

The above mentioned requirements will be satisfied if the modal frequencies will be modified as

$$[\mathrm{diag}(0, \ldots, 0, \alpha^\omega_{r+1}\omega^2_{r+1}, \alpha^\omega_{r+2}, \omega^2_{r+2}, \ldots, \alpha^\omega_{r+n}\omega^2_n)] = [\mathrm{diag}(\omega^2)]\{\boldsymbol{\alpha}^\omega\} \tag{7}$$

and the modal shapes modified as

$$[\{\tilde{\mathbf{y}}_1\}, \ldots, \{\tilde{\mathbf{y}}_r\}, \alpha^y_{r+1}\{\tilde{\mathbf{y}}_{r+1}\}, \ldots, \alpha^y_n\{\tilde{\mathbf{y}}_n\}] = [\tilde{\mathbf{Y}}]\{\boldsymbol{\alpha}^y\} \tag{8}$$

where $\{\boldsymbol{\alpha}^\omega\}^\mathrm{T} = \{1, \ldots, 1, \alpha^\omega_{r+1}, \ldots, \alpha^\omega_n\}$, $\{\boldsymbol{\alpha}^y\}^\mathrm{T} = \{1, \ldots, 1, \alpha^y_{r+1}, \ldots, \alpha^y_n\}$ are coefficients the values of most of which are close to unity.

Finally, we reformulate the above mentioned Problem 1 as follows: *Find the values of coefficients $\{\boldsymbol{\alpha}^\omega\}$, $\{\boldsymbol{\alpha}^y\}$ and β^l_i, $i = 1, \ldots, n$, determining the modal properties of a single component domain that minimize errors of modal frequencies of the joined domain obtained by joining together several component domains*.

Consider a joined domain presented by structural matrices of dimension $\hat{N} \times \hat{N}$ as $[\hat{M}]_{\hat{N}\times\hat{N}}$, $[\hat{\mathbf{K}}]_{\hat{N}\times\hat{N}}$ assembled of component domain matrices $[\tilde{\mathbf{M}}]_{n\times n}$, $[\tilde{\mathbf{K}}]_{n\times n}$. The solution of the eigen-value problem of the joined domain gives the modal frequencies $\hat{\omega}_1, \hat{\omega}_2, \ldots, \hat{\omega}_{\hat{N}}$ and modal shapes $[\hat{\mathbf{Y}}] = [\{\hat{\mathbf{y}}_1\}, \{\hat{\mathbf{y}}_2\}, \ldots, \{\hat{\mathbf{y}}_{\hat{N}}\}]$.

The modal frequency error minimization problem can be formally presented as

$$\min_{\{\boldsymbol{\alpha}^\omega\}, \{\boldsymbol{\alpha}^y\}, \beta^l_k} \Psi \tag{9}$$

where the penalty-type target function presents the cumulative modal frequency error and reads as

$$\Psi = \sum_{i=r+1}^{\hat{N}} \left(\frac{\hat{\omega}_i - \hat{\omega}_{i0}}{\hat{\omega}_{i0}} \right)^2$$

where $\hat{\omega}_i$—modal frequency of ith mode of the joined domain, $\hat{\omega}_{i0}$—exact value of the modal frequency of ith mode, known theoretically or obtained by using a highly refined finite element model.

To solve (9) for a real computational domain in a general case seems to be rather expensive and hardly reasonable. In reality we do not try to optimize the domain matrices by assembling

the matrices of the whole real computational domain. A reasonable choice is to perform optimization by assembling component domains into *sample domains* the modal frequencies of which are known, and then to use the obtained matrices of component domains for assembling the real computational domains. We did not present any theoretical proof of the validity of this approach, however, numerical experiments illustrate that it works.

Good results may be achieved by improving the component domain matrices step by step as follows

(1) A sample domain of a regular shape (linear, rectangular, triangular) is selected, the sufficiently large number of exact modal frequencies of which is known. For example, for linear and rectangular elastic and acoustic domains such modal frequencies are available analytically. In other cases a highly refined model of the sample domain can be used in order to obtain 'nearly exact' (say, $< 0.5\%$) modal frequency values.

(2) If the sample domain is represented by a single roughly meshed component domain, the solution $\{\boldsymbol{\alpha}^\omega\} = 1$, $\{\boldsymbol{\alpha}^y\} = 1$, $\beta_i^l = 1$, $i = 1, \ldots, n$ ensures the minimum of the target function as $\Psi = 0$.

(3) The sample domain is represented by two component domains and problem (9) is being solved by taking the solution obtained in step 2 as an initial approximation. As a result, new values of $\{\boldsymbol{\alpha}^\omega\}$, $\{\boldsymbol{\alpha}^y\}$, β_i^l, $i = 1, \ldots, n$ are obtained.

(4) After that we analyse the sample domain made of three and more component domains, etc.

The number of such optimization steps is practically determined by a reasonable amount of calculations. Our numerical experiments demonstrate that for uni-dimensional case it is enough to perform optimization on the joined domain consisting of only three component domains, and the optimized matrices of a single component domain work well if a considerably larger structure is assembled.

Optimization calculations are rather expensive. If the sample domain consists of more than one component domains, the minimum of the target function Ψ is not easy to find. The target function minimization process can be facilitated by calculating the derivatives of function Ψ with respect to variables $\{\boldsymbol{\alpha}^\omega\}$, $\{\boldsymbol{\alpha}^y\}$, $\beta_i^l = 1$, $i = 1, \ldots, n$. The vector containing the full set of the derivatives is called as the gradient of function Ψ which is used as the search direction.

For implementing the optimization method based on the gradient, the sensitivity functions

$$\frac{\partial \Psi}{\partial \{\boldsymbol{\alpha}^\omega\}}, \frac{\partial \Psi}{\partial \{\boldsymbol{\alpha}^y\}}, \frac{\partial \Psi}{\partial \beta_j^l}, \quad j = 1, \ldots, n$$

are employed. The gradient calculation techniques when applied to structural dynamics optimization problems are thoroughly discussed in the fundamental work [12]. The basic variation relations for obtaining the gradient read as

$$\partial \Psi = \sum_{i=1}^{\hat{N}} \frac{\hat{\omega}_i - \hat{\omega}_{i0}}{\hat{\omega}_{i0}^2 \hat{\omega}_i} \delta \hat{\omega}_i^2 \tag{10}$$

$$\delta \hat{\omega}_i^2 = \{\hat{\mathbf{y}}_i\}^{\mathrm{T}} \left(\frac{\partial [\hat{\mathbf{K}}]}{\partial \alpha} - \omega_i^2 \frac{\partial [\hat{\mathbf{M}}]}{\partial \alpha} \right) \{\hat{\mathbf{y}}_i\} \delta \alpha; \quad \alpha = \alpha_j^y, \alpha_j^\omega, \beta_j^l, \quad j = 1, \ldots, n \tag{11}$$
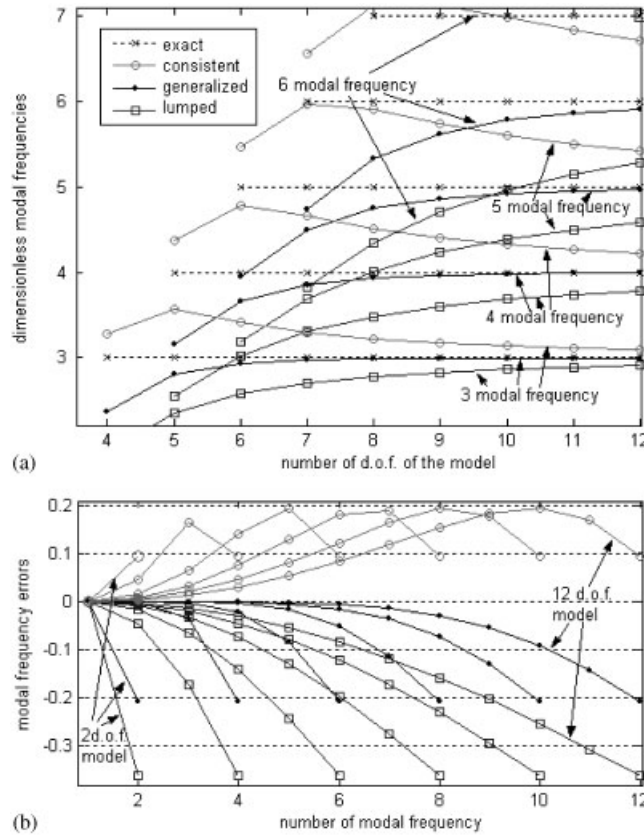
Figure 2. (a) Modal frequencies of the same uni-dimensional domain against the number of DOF of the model; and (b) relative modal frequency errors. Positions of markers correspond to modal frequencies.

5. NUMERICAL INVESTIGATIONS

5.1. Dynamic properties of models using lumped, consistent and generalized mass matrices of a uni-dimensional waveguide

We begin the modal convergence analysis with the uni-dimensional waveguide models. Modal frequencies of the same uni-dimensional domain obtained by using models of different mesh density are presented in Figure 2.

Each curve in Figure 2(a) demonstrates how the value of a particular modal frequency depends upon the number of DOF of the model. By increasing the number of DOF, the curves are asymptotically approaching the dashed lines marked by crosses that present theoretical values of modal frequencies obtained as $\omega_{i0} = \pi(i-1)/l\sqrt{E/\rho}$, where E, ρ—stiffness modulus and density of the material, l—length of the waveguide, i—number of the mode. Markers on the same solid line correspond to frequencies of different modes obtained by using the same model.

The lumped mass matrix $[\mathbf{M}_\mathrm{L}]$ models always give diminished values of modal frequencies, whereas the consistent mass matrices $[\mathbf{M}_\mathrm{C}]$ always cause the oversized values. Generally, the behaviour of models using the generalized mass matrix $[\mathbf{M}] = k_\mathrm{C}[\mathbf{M}_\mathrm{C}] + k_\mathrm{L}[\mathbf{M}_\mathrm{L}]$ depends upon the weight coefficient values $k_\mathrm{C}, k_\mathrm{L}$. Here we present the results obtained by using one of reasonable choices of the generalized mass matrix ($k_\mathrm{C} = 0.53$; $k_\mathrm{L} = 0.47$) ensuring the minimum relative error of lower and middle modal frequencies. In order not to overload the picture, only modal frequencies of the 3rd, 4th, 5th and 6th modes are presented in Figure 2(a) for models using lumped, consistent and generalized forms of the mass matrix. However, the same character of relationships holds for all remaining modes as well. The left-hand end of each curve in Figure 2(a) presents the highest modal frequency obtainable by using the model of the particular dimension.

The relative modal frequency errors as $(\omega_i - \omega_{i0})/\omega_{i0}$ may be examined in Figure 2(b). The error of the zero-mode ($i = 1$) is negligible in the case of any form of the mass matrix as the eigenvalue very close to zero is always obtained because of the singular stiffness matrix of an unsupported structure. It is interesting to note that the relative errors of the very highest frequency given by using models of any dimension are constant and individual for each form of the mass matrix. The values of the highest modal frequency errors are $\sim 37\%$ for the lumped mass matrix and only $\sim 10\%$ for the consistent one. However, the maximum errors ($\sim 20\%$) obtained by using the consistent matrices are in the middle modal frequency range rather in the higher one. Very similar modal frequency error values in the middle frequency range are obtained also by using the lumped mass matrix. Though the total modal frequency error of consistent mass matrix models is less than of the lumped ones, practically both models produce very similar level of errors in the wave pulse propagation modelling.

The performance of the considered models in short wave pulse propagation modelling is illustrated in Figure 3. For the sake of comparison in Figure 3(a) the 'exact' solution is presented. Practically, the solution obtained by using a dense mesh (~ 35 nodes per wavelength) can be reasonably treated as exact one for comparison purposes in order to evaluate the accuracy of solutions obtained in coarser meshes. The shape of the wave is presented at the time point of the fourth passage of the wave along the waveguide (the wave is three times refracted from the ends of the waveguide, see the scheme of the 'path of the wave' at the top of the figure). In our computations we used the central difference time integration scheme with the CFL number $c\Delta t/\Delta x \approx 0.1$, where c—wave propagation velocity, Δt, Δx—time and space step sizes. Every result has been checked for convergence of the time integration scheme by recalculating it with twice less time step and comparing the results for coincidence. Therefore the distortions of wave pulses presented here are caused by spectral properties of the discrete model and surely not because of the time integration errors.

In Figures 3(b) and (c) the distorted wave pulse shapes corresponding to the lumped and consistent mass matrix models are presented. The character of distortions is different in each case. The lumped mass matrix models are inclined to generate the numerical noise that follows the main signal, whereas the consistent matrix models produce the numerical noise propagating in front of the pulse. However, the amount of distortion is very similar. A rough mesh having 12 nodes per pulse length has been selected for demonstrating the behaviour of the models in order to make the distortions clearly visible. The same characteristic numerical noise is more or less observed in models of any mesh roughness. The generalized mass matrix models produce errors presented by lines marked by dots in Figure 2(b). While having errors of $\sim 20\%$ for the very highest frequency, their modal frequency errors in lower and middle frequency range are
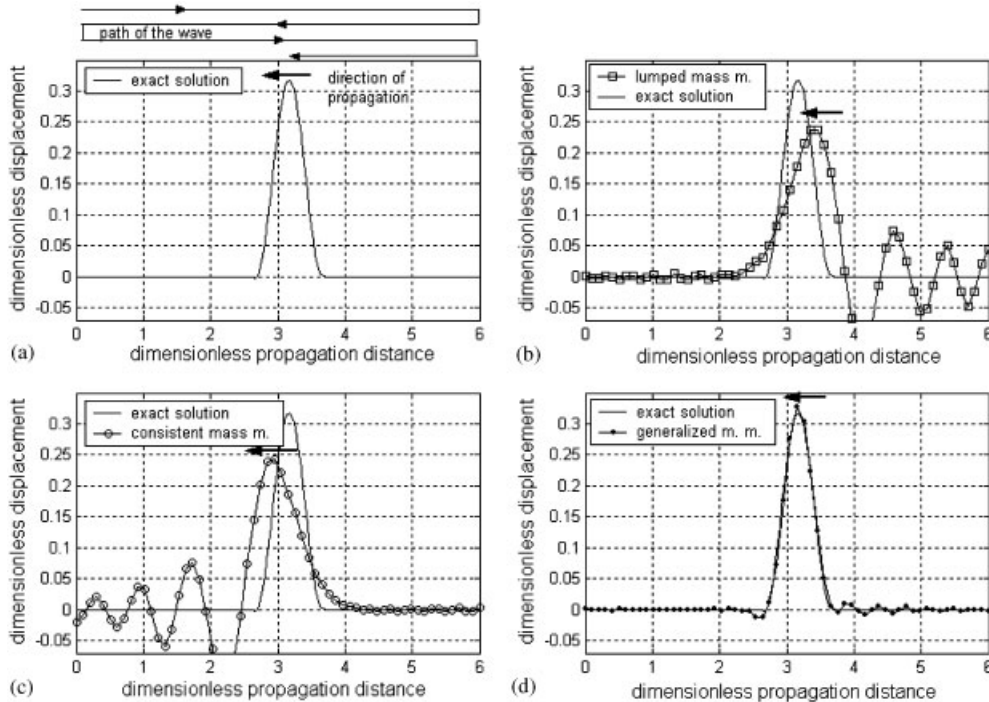
Figure 3. Typical distortions of the shape of a propagating wave pulse in a rough equally spaced mesh: (a) 'exact' solution of a propagating wave pulse excited by one period of harmonic forcing law at the left-hand end of the waveguide; (b) obtained by using roughly meshed model (12 modal points per wavelength) with the lumped mass matrix; (c) obtained by using roughly meshed model with the consistent mass matrix; and (d) obtained by using roughly meshed model with the generalized mass matrix as $[\mathbf{M}^e] = 0.53[\mathbf{M}^e_C] + 0.47[\mathbf{M}^e_L]$.

about 10 times less when compared with the two traditional models. The practical result of this can be seen in Figure 3(d) demonstrating the distorted pulse shape at the same propagation conditions and mesh density as in Figures 3(b) and (c). As mentioned above, here we analyse the mesh density of 12 nodes per wave pulse length excited by a single period of a harmonic signal (note that the frequency of the highest harmonic component participating in presenting the single-period shaped pulse is at least three times greater than the main frequency). So, in reality we used only ~ 4 nodes per shortest wavelength. The pulse shown in Figure 3(d) is still distorted by a certain amount (though quite small) of the leading and lagging noise (compare with the 'exact' version of the pulse in Figure 3(a)). By changing the values k_C, k_L the amounts of the leading/lagging noise can be changed. What is presented in Figure 3(d) is nearly the 'optimum', at least from the visual inspection standpoint. It demonstrates clearly that the effect of using generalized matrices is really considerable.

The behaviour of the errors is actually consistent with the phase velocity errors in the mid-range of the discrete spectrum. The phase velocity is the velocity with which the harmonic wave of a certain frequency is travelling along the waveguide and is defined as $v_f = \omega/k$, where ω is the wave frequency, and k is the wave number. The expression holds in the case of a
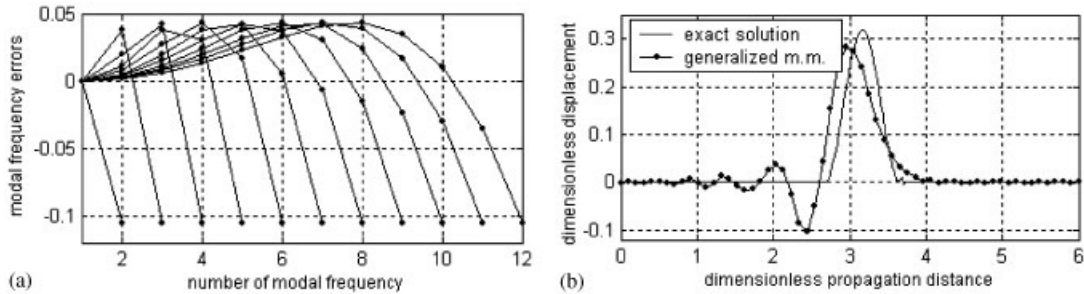
Figure 4. (a) Relative modal frequency errors of an uni-dimensional waveguide; and (b) distortion of a propagating wave pulse in the case of the generalized mass matrix $[\mathbf{M}] = 0.74[\mathbf{M_C}] + 0.26[\mathbf{M_L}]$ minimizing the cumulative (SRSS) relative modal error.

standing wave that may be expressed as a superposition of the propagating and reflected waves. In the same way the phase velocity of the ith mode is defined as $v_{fi} = \omega_i/k_i$, where ω_i is the modal frequency, and the wave number k_i is established by analysing the corresponding modal shape. So, in finite element-based wave propagation models the phase velocities of different modes are slightly different from the exact values mostly because of the modal frequency errors. Therefore different harmonic components of the same wave pulse are traveling through the model with different phase velocities and do not arrive to some considered point at the same time. As a result, after some propagation time the pulse shape is distorted and also the 'noise' in front of and(or) behind the pulse appears.

The total modal frequency error can be minimized by choosing the values of coefficients $k_C = 0.74$; $k_L = 0.26$. However, the results presented in Figure 4 demonstrate that the model gives much greater pulse shape distortion as in the case $k_C = 0.53$; $k_L = 0.47$ presented in Figure 3(d). Obviously, it is much better to ensure negligible modal frequency errors in low and middle frequency range than to 'distribute' the error among all modes. The latter conclusion can be considered as a general one and may be used for establishing the modal frequency error minimization criteria for all types of the synthesized mass matrices.

5.2. Properties of models using lumped, consistent and generalized mass matrices of an acoustic problem in a square shaped closed cavity

As a two-dimensional example we present the modal frequency error relationships for the acoustic problem formulated in a square shaped closed cavity. The exact modal frequencies can be expressed as

$$\omega_{(m,n)0} = \pi\sqrt{\frac{E}{\rho}}\sqrt{\left(\frac{m}{a}\right)^2 + \left(\frac{n}{b}\right)^2}$$

where a, b–lengths of the sides of the rectangular. Here the square domain is being analysed, $a = b$. The basic properties of models described by using different forms of mass matrices are briefly explained in Figure 5. Relative modal frequency errors of the square domain obtained by using the consistent, lumped and generalized mass matrices are presented in Figure 5(a). Qualitatively, the general character of the curves is very close to the results obtained for a uni-dimensional domain presented in Figure 2(b). Evidently, there exists an optimum weighted

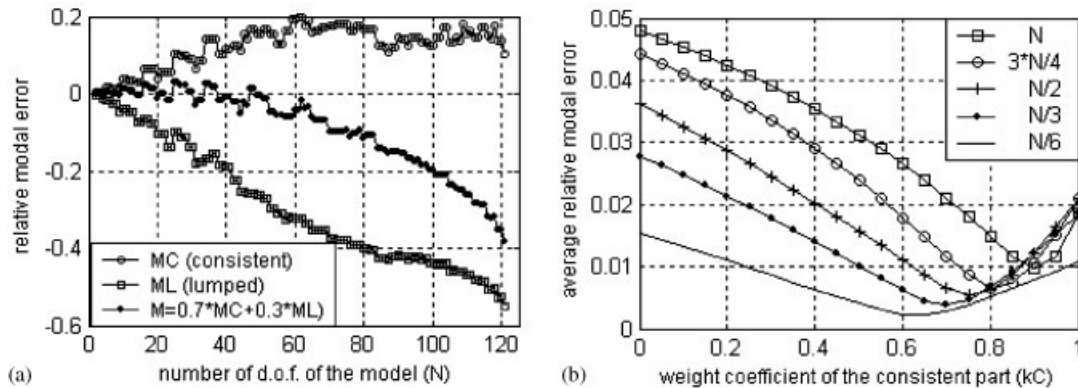*Int. J. Numer. Meth. Engng* 2004; **61**:2536–2554

Figure 5. (a) Modal frequency errors of an acoustic problem in 2D square shaped closed cavity; and (b) relationships of average relative errors of modal frequencies against the weight coefficient of the consistent component.

combination of the generalized and lumped matrices $[\mathbf{M}] = k_C[\mathbf{M}_C] + k_L[\mathbf{M}_L]$. The reasoning for the choice of value k_C can be understood from Figure 5(b), where the relationships of average modal frequency error taken as square root of sum of squares

$$\frac{1}{N}\sqrt{\sum_{i=1}^{N}\left(\frac{\omega_i - \omega_{i0}}{\omega_{i0}}\right)^2}$$

against the value k_C are presented. Each curve describes the cumulative error values obtained by taking sums over a different number of modes: N (summation over all modes), $3*N/4$, $N/2$, etc. As it is impossible to get very small error values over all modal frequency range, the optimum values of k_C are slightly different in each case. Practically, for minimum numerically caused distortion of propagating wave pulses a reasonable choice is $k_C = 0.7$, $k_L = 1 - k_C = 0.3$.

5.3. Optimization of the modal spectrum of component domains

Consider a wave pulse propagating along a uni-dimensional elastic waveguide. The finite element model of the waveguide consists of NSUB uni-dimensional component domains joined at their ends. The domains are all identical and presented by stiffness and mass matrices obtained by using the modal synthesis technique described in Section 3. Examine the dynamic properties of models of approximately the same size NT ≈ 60 dynamic DOF obtained by joining together component domains the number of DOF of each is n such that NT $= (n-1) \times$ NSUB $+1 \approx 60$. It means, we analyse the model consisting of the single domain containing $n = 60$ dynamic DOF, or assembled of two domains containing $n = 31$ dynamic DOF each, or made of 3 domains containing $n = 21$ dynamic DOF each, etc (Figure 6).

The aim of investigation is to synthesize matrices of component domains producing the 'optimum' modal frequency errors of joined domains (as discussed in Section 5.1, minimum cumulative error is not the optimum) ensuring as small as possible distortions of propagating wave pulses. The ultrasonic pulse is being excited at the left-hand end by the force developed
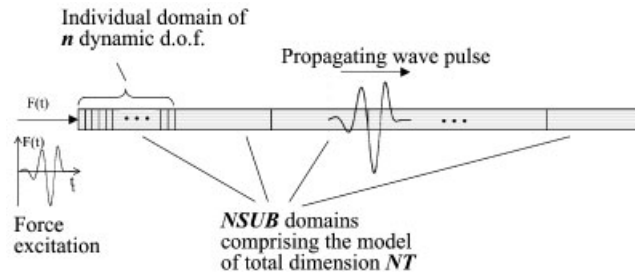
Figure 6. Scheme of a uni-dimensional wave pulse propagation model
made of NSUB component domains.

by the input transducer. As a rule, the width of the spectrum of pulses usually used ultrasonic measurements contain harmonic components up to $2.5 - 3\omega$, where ω—the frequency of the main harmonic component of the pulse.

For illustrating the basic ideas we consider a uni-dimensional waveguide model (64 nodes in total) assembled of 7 component domains having 10 nodes each. Optimization of matrices has to be performed on the base of the penalty-type target function of the domain assembled of at least 3–4 component domains or more. Optimization of matrices of large component domains is a time consuming task as the modes of all joined domain have to be calculated at each optimization step.

In Figure 7 modal frequency errors $(\hat{\omega}_i - \hat{\omega}_{i0})/\hat{\omega}_{i0}$ of the waveguide model are presented. As described in Section 4, component domains having all modal frequencies equal to their exact (theoretical) values are obtained by taking the modal frequency and modal shape correction coefficient values as $\alpha_i^\omega = \alpha_i^y = \beta_i^1 = 1$. However, such component domain matrices assembled to a joined domain produce poor results. Figure 7(a) demonstrates the up to 4% modal frequency error values of the joined domain distributed over all modal frequency range. If more component domains are used to form the joined domain, modal frequency errors increase even more and the model performs worse than the models using the generalized mass matrix.

The modal frequency error of the joined domain is minimized by using the method described in Section 4. If the matrices of 10-node component domains are designed in order to ensure the minimum of the target function $\Psi = \sum_{i=1}^{64} ((\hat{\omega}_i - \hat{\omega}_{i0})/\hat{\omega}_{i0})^2$ (i.e. by taking the sum over $\hat{N} = 64$ modes of the joined domain), we obtain the result presented in Figure 7(b). It is clear that the eight higher modal frequency values (comprising about 12% of the total number of modes of the model) cannot be made close enough to the theoretical ones. Even better results are obtained by carrying out the optimization process of the target function where the sum is taken over only $\hat{N} = 55$ modes, see Figure 7(d). The minimization parameters are α_i^ω; α_i^y; $\beta_i^l, i = 2, \ldots, \hat{N}$. The non-unity α_i^ω values mean that the component domains have to have the modal frequencies not equal to the theoretical ones. If we enforce the requirement $\alpha_i^\omega = 1$ and carry out the optimization only in space of parameters α_i^y; $\beta_i^l, i = 2, \ldots, \hat{N}$, the result is presented in Figure 7(c) and is significantly worse than the one in Figure 7(d). The detuning of modal frequencies of the component domain from their theoretical values can be regarded as an inherent requirement for synthesizing optimum dynamic models.

It is very important that the optimized component domain models preserve their features when being used in a joined domain models of any dimension. Without any theoretical proof
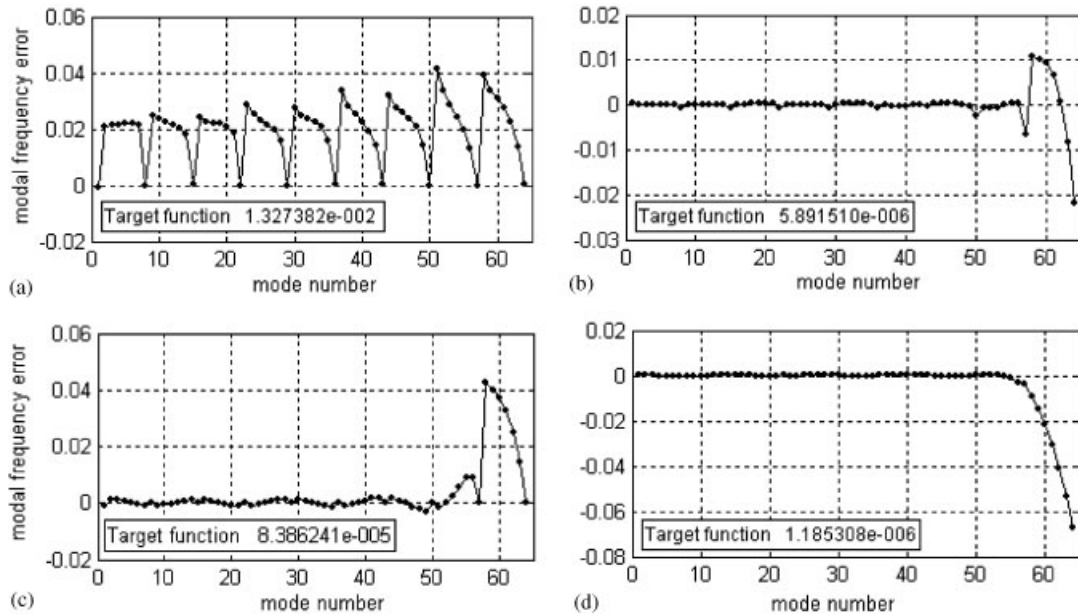
Figure 7. Modal frequency errors of a uni-dimensional waveguide model (64 nodes in total) assembled of 7 component domains of 10 nodes each: (a) non-optimized case: matrices of component domains obtained by using coefficient values $\alpha_i^e = \alpha^y = \beta_i^l = 1$; (b) optimized by taking the sum over all $\hat{N} = 64$ modal frequencies of the joined domain; (c) optimized by taking the sum over all $\hat{N} = 55$ modal frequencies of the joined domain (exact modal frequencies of the component domain preserved); and (d) optimized by taking the sum over all $\hat{N} = 55$ modal frequencies of the joined domain (modal frequencies of the component domain detuned from their theoretical values).

we merely present illustration of this in Figure 8, where the obtained 10-node component domains were used in order to make the joined domains of different size. The distribution of modal frequency errors over all the modal frequency range and the percentage of error-free modes is independent from the dimension of the joined domain, therefore component domain matrices can be treated as high order well-convergent elements.

Figure 9 presents the modal frequency errors of a joined domain assembled of optimized component domains of different size. The advantage of synthesized component domains in comparison with the generalized mass matrix is obvious. The generalized mass matrix models are able to produce about 35% error free modal frequencies of the joined domain, meanwhile the models based upon 10-node component domains provides 86% of error free modal frequencies. On the other hand, not all the sizes of component domains can be optimized to give the result of the same quality. E.g. in our investigations we distinguished component domains of dimension 5 and 10 as producing the highest percentage of error free modes. The increase of the component domain dimension to 15, 20 and 30 does not give any advantage as the percentage of correctly represented modes in joined domains does not increase any more, see Figure 9(b).
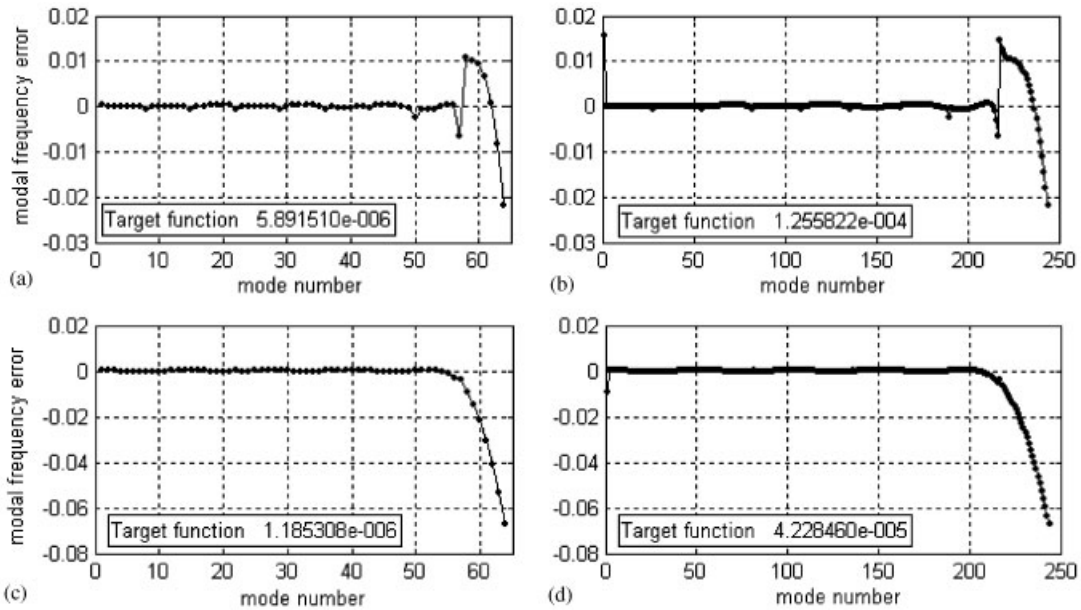
Figure 8. Modal error distribution in joined domains assembled of 6 (a and c) and 24 (b and d) 11-node component domains presented by optimized matrices: 6 (a), (b)—optimized by taking the sum over all $\hat{N} = 64$ modal frequencies of the joined domain; and 6 (c), (d)—optimized by taking the sum over all $\hat{N} = 55$ modal frequencies of the joined domain.
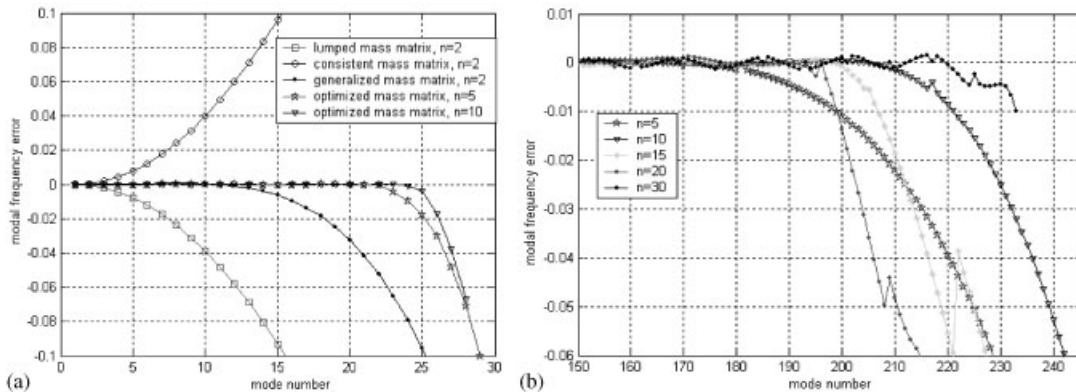

Figure 9. Modal errors of a joined domain assembled of several component domains: (a) 30 DOF models assembled of humped, consistent, generalized mass matrices and optimized component domains of dimension $n = 5$ and 10; and (b) 240 DOF models assembled of component domains of dimension $n = 5$, 10, 15, 20 and 30.
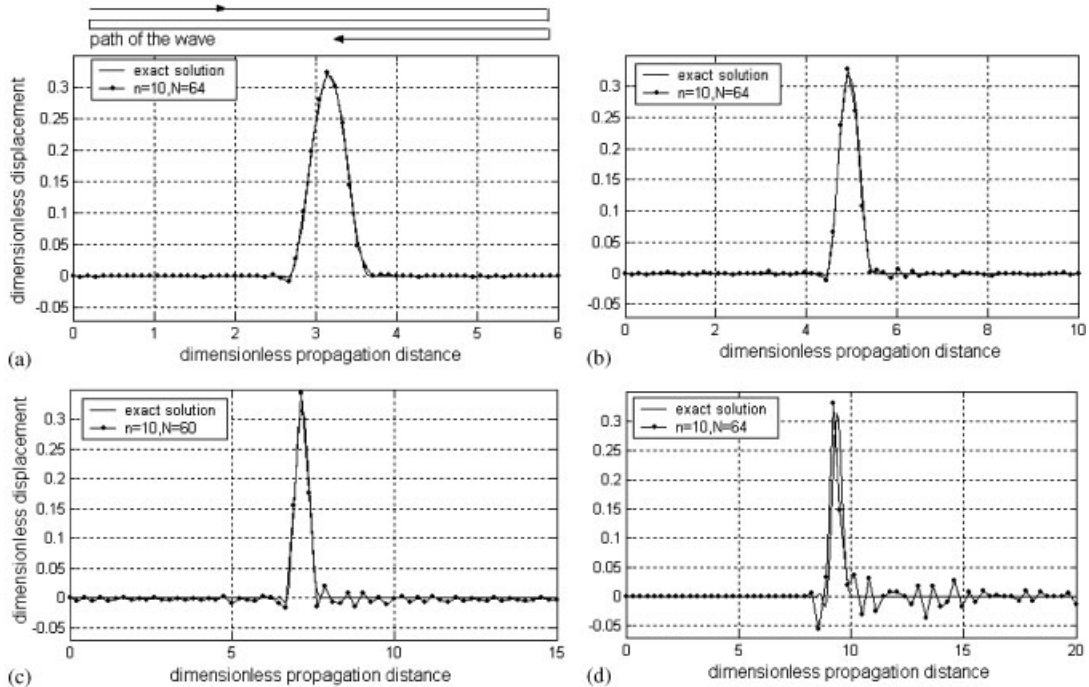
Figure 10. Shape distortion of a propagating wave pulse in the model assembled of seven 10-node component domains length. Nodes of the mesh per pulse length: (a) 12 nodes; (b) 7 nodes; (c) 5-nodes; and (d) 4 nodes.

The performance of the 10-node component domain used in the 64 nodes model of the waveguide simulating the wave pulse propagation is presented in Figure 10. The figure presents the shape distortion of the propagating wave pulse after ~ 3.5 passages through the joined domain of the waveguide (see the path of the wave at the top of Figure 10(a)). 12 or even 7 nodes per pulse length are enough for simulating the pulse propagation over quite a large distance, Figure 10(a) and (b). The model actually works satisfactorily also at very rough meshes of 5 or 4 points per pulse length, Figure 10(c) and (d). At the same conditions, the conventional lumped or consistent mass matrix models produce the numerical noise larger then the signal itself and no resemblance of the pulse shape would be seen in the picture.

6. CONCLUSIONS

A regular approach has been presented for obtaining the mass and stiffness matrices of component domains such that after assembling the component domain matrices to a larger model the convergence of modal frequencies is as high as possible. The method is based upon the minimization of the modal frequency errors of some selected sample domains and then using the obtained component domain matrices for assembling the real computational domains. The best performance is obtained by using the component domains the modal frequency spectrum

of which is appropriately detuned from their theoretical values. The obtained mass matrices are non-diagonal. Once calculated, the component domain matrices can be used to form any structure and may be interpreted as higher-order elements or super-elements. The latter result has not been proved theoretically, however, illustrated by numerical examples.

When compared with lumped, consistent or generalized mass matrices, the matrices obtained by modal synthesis and optimization produce significantly better results. The models able to present very close-to-exact (less than 0.5% error) modal frequency values of more than ∼80% of the total modal frequency number can be obtained. Though the method is illustrated basically by means of uni-dimensional examples, it is formulated for 2D and 3D domains as well.

The obtained dynamic models can be used primarily for modelling short transient waves and wave pulses propagating in elastic or acoustic environments. The distinguishing feature of such models is their ability to present the wave pulse by using very few nodal points per wavelength.

The natural limitation of the presented approach is that it is oriented to produce very efficient discrete models of large uniform zones of structures in which the wave propagation is investigated. Actually, the most efficient application may be found in implementing models based on the domain decomposition, where large uniform domains can be presented by means of rough meshes and considerable computational resource savings may be obtained. In irregular zones they can be joined with conventional finite element meshes. The matrices of each component domain are fully populated, and any transformation of them to the diagonal form can make the modal convergence worse. Therefore a reasonable choice is to use well-optimized small component domains.

REFERENCES

 1. Mullen R, Belytschko T. Dispersion properties of finite element semi-discretizations of the two-dimensional wave equations. *International Journal for Numerical Methods in Engineering* 1982; **18**:1–29.
 2. Daniulaitis V, Barauskas R. Modelling techniques for ultrasonic wave propagation in Solids. *Ultragarsas* 1998; **1**(29).
 3. Christon MA. The influence of the mass matrix on the dispersive nature of the semi-discrete, second-order wave equation. *Computer Methods in Applied Mechanics and Engineering* 1999; **173**:147–166.
 4. Jensen MS. High convergence order finite elements with lumped mass matrix. *International Journal for Numerical Methods in Engineering* 1996; **39**:1879–1888.
 5. Hanson P, Sandberg G. Mass matrices by minimization of modal errors. *International Journal for Numerical Methods in Engineering* 1997; **40**:4259–4271.
 6. Haug EJ, Pan W. Optimal inertia lumping from modal mass matrices for structural dynamics. *Computer Methods in Applied Mechanics and Engineering* 1998; **163**:171–191.
 7. Laier EL. Hermitian lumped mass matrix formulation for flexural wave propagation. *Communications in Numerical Methods in Engineering* 1998; **14**:43–49.
 8. Rozenblum G. Modal synthesis: generalization of MacNeal's method. Theoretical basis. *Computer Methods in Applied Mechanics and Engineering* 1985; **48**:139–154.
 9. Qiu J-B, Ying Z-G, Williams FW. Exact modal synthesis techniques using residual constraint modes. *International Journal for Numerical Methods in Engineering* 1997; **40**:2475–2492.
10. Shechter RS, Chaskelis HH, Mignona RB, Delsanto PP. Real-time parallel computation and visualization of ultrasonic pulses in solids. *Science* 1994; **265**:1188–1192.
11. Hughes TJR. *The Finite Element Method*. Prentice-Hall: Englewood Cliffs, NJ, 1987.
12. Haug EJ, Arrora JS. *Applied Optimal Design*. Wiley: New York, 1979.